



0008-6223(95)00216-2

FACTORS LIMITING THE TENSILE STRENGTH OF PBO-BASED CARBON FIBERS

J. A. NEWELL^a and D. D. EDIE^b^aDepartment of Chemical Engineering, University of North Dakota, Grand Forks, ND 58202-7101, U.S.A.^bDepartment of Chemical Engineering and Center for Advanced Engineering Fibers, Clemson University, Clemson, SC 29634-0909, U.S.A.

(Received 23 January 1995; accepted in revised form 13 October 1995)

Abstract—Poly *p*-phenylene benzobisoxazole (PBO) converts directly to carbon fiber without stabilization. However, the applicability of PBO-based carbon fibers is limited by their low tensile strength. This paper represents the first study of the high-temperature conversion of PBO to carbon fiber and examines some factors leading to this low tensile strength. A mixed-mode Weibull analysis implies that the flaws present in the precursor fiber persist throughout carbonization and cause the tensile failure of the carbonized fiber. Improvements in the PBO spinning process resulted in increased tensile strengths for the carbonized fibers. Further, the tensile strengths of the carbonized fibers appear to be related to the release of nitrogen during the onset of crystallite growth. The rapid heating rates associated with continuous carbonization were shown to minimize the negative effects of this nitrogen release. Fibers heated to 1600°C in a continuous operation displayed nearly double the tensile strength of those produced in a batch operation. Ultimately, this study showed that, while the tensile strengths of PBO-based carbon fibers can be increased by using a continuous process, enhancements in the solution spinning process of the polymer will be required for PBO to become a commercially viable carbon fiber precursor. Copyright © 1996 Elsevier Science Ltd

Key Words—Poly *p*-phenylene benzobisoxazole, Weibull, PBO.

1. INTRODUCTION

The primary factor limiting the widespread commercial use of carbon fibers is their high production cost. A significant portion of this cost is a direct result of the lengthy stabilization that traditional precursor materials require [1]. Poly *p*-phenylene benzobisoxazole (PBO) fibers have been shown to convert directly to carbon fiber without stabilization [2], which dramatically reduces the cost of processing. Table 1 shows that the tensile moduli and electrical resistivities of PBO-based carbon fibers compare favorably with those of carbon fibers made from pitch and PAN (polyacrylonitrile). However, the use of PBO-based carbon fibers currently is limited by their substandard tensile strengths. To enhance the tensile strength of PBO-based carbon fiber, it is essential to understand the causes of failure.

Tensile failure could result from flaws in the precursor fiber, damage created during carbonization, or a combination of the two factors. The molecular struc-

ture of PBO, shown in Fig. 1, provides some insight. The nitrogen in the oxazole ring is bound similarly to the nitrogen in stabilized PAN fibers. Previous studies [3–5] have concluded that the high-temperature release of nitrogen disrupts the developing crystalline order of the fiber, which leads to a decrease in tensile strength.

If the damage associated with nitrogen release results in the poor tensile strength of the PBO-based carbon fiber, heating the fiber at accelerated rates should minimize the deleterious effects. Rapid heating through the region of nitrogen release provides less time at elevated temperatures for crystallite growth, thereby minimizing the destructive effects of the nitrogen release. Similar behavior has been described in the literature for the high-temperature release of sulfur from mesophase pitch-based fibers [6].

By contrast, observation and quantification of the role of precursor flaws is not as direct. Microscopic flaws cause tensile failure to occur below the intrinsic strength of the fiber [7]. Therefore, analysis of tensile failure data should provide insight into the distribution of flaws within the fiber. The fiber may be viewed as a chain of interlocking links, with the flaws acting

Table 1. Properties of carbon fibers

Precursor Material	Product Designation	Tensile Strength (GPa)	Tensile Modulus (GPa)	Electrical Resistivity ($\mu\Omega\cdot\text{m}$)
PAN	T-300	3.65	231	18
Pitch	P-55	1.90	415	9
PBO	Batch-1400	0.73	180	11
	Batch-1800	0.52	245	13
	Cont.-1400	1.05	175	14
	Cont.-1800	0.85	183	10

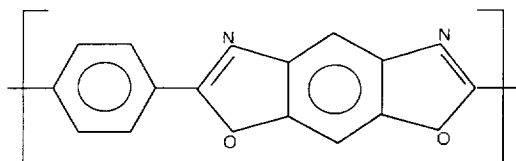


Fig. 1. The repeat unit of PBO.

as "weak links" in the chain. Ultimately, the chain will fail at its weakest link.

Tensile data do not conform to rigid statistical distributions. Thus, they cannot be represented accurately by fixed statistical distributions. Instead, it is necessary to use a flexible distribution that enables the shape of the distribution function to be altered by the data itself. The Weibull distribution normally is preferred for analyzing carbon fiber data [8].

The Weibull cumulative distribution function takes the form

$$F_i = 1 - \exp\left(-\left(\frac{\sigma}{\sigma_0}\right)^m\right) \quad (1)$$

where F_i is the probability of a given link failing at or below a given stress level, σ is the applied stress level, σ_0 is a scale factor which represents the severity of flaws and m is the shape factor which relates to the distribution of flaws. The probability of survival (S_i) for any link then is given by

$$S_i = 1 - F_i \quad (2)$$

When eqn (1) is substituted into the above equation, the probability of survival becomes

$$S_i = \exp\left(-\left(\frac{\sigma}{\sigma_0}\right)^m\right) \quad (3)$$

If any individual link fails, the entire fiber will fail. Therefore, the probability of survival for a fiber of gauge length (L) is the product of the survival probabilities for each link in that length of fiber.

$$S = \prod_{i=1}^L S_i \quad (4)$$

The assumptions that each link fails or survives independently of its neighbors and that the strength of each link can be represented by a single Weibull distribution enables eqn (4) to be rewritten as

$$S = (S_i)^L \quad (5)$$

Substituting eqn (3) into eqn (5) yields

$$S = \exp\left(-L\left(\frac{\sigma}{\sigma_0}\right)^m\right) \quad (6)$$

Because the fiber must either survive or fail, the probability of failure at a given stress level becomes

$$F = 1 - \exp\left(-L\left(\frac{\sigma}{\sigma_0}\right)^m\right) \quad (7)$$

where L is the length of fiber being tested.

For cases in which the simple Weibull distribution fails to provide an adequate representation of the data, mixed failure mode distributions must be considered. The two most relevant mixed distributions are a concurrent failure model and an end-effect failure model [9,10]. In these models, two independent distributions (one for flaw type 1 and another for flaw type 2) combine to control the overall distribution of failures, instead of a single flaw distribution controlling tensile strength.

In the concurrent model, each flaw distribution

obeys the same form as in the simple Weibull case

$$S_1 = \exp\left(-L\left(\frac{\sigma}{\sigma_{0_1}}\right)^{m_1}\right) \quad (8)$$

$$S_2 = \exp\left(-L\left(\frac{\sigma}{\sigma_{0_2}}\right)^{m_2}\right) \quad (9)$$

However, four constants (σ_{0_1} , σ_{0_2} , m_1 , and m_2) now must be fit to represent the data. Each flaw population contributes to fiber failure, and thus, the fiber must survive both populations in order to withstand a given level of stress. Therefore, the probability of survival becomes the product of the probabilities of surviving each individual flaw population

$$S = \exp\left(-L\left(\frac{\sigma}{\sigma_{0_1}}\right)^{m_1}\right) \exp\left(-L\left(\frac{\sigma}{\sigma_{0_2}}\right)^{m_2}\right) \quad (10)$$

or more conveniently,

$$S = \exp\left(-L\left(\frac{\sigma}{\sigma_{0_1}}\right)^{m_1} - L\left(\frac{\sigma}{\sigma_{0_2}}\right)^{m_2}\right) \quad (11)$$

Because the fiber must either survive or fail, the probability of failure becomes

$$F = 1 - \exp\left(-L\left(\frac{\sigma}{\sigma_{0_1}}\right)^{m_1} - L\left(\frac{\sigma}{\sigma_{0_2}}\right)^{m_2}\right) \quad (12)$$

By contrast, the end-effect model assumes that the atypical stress distribution at the fiber–glue interface causes some fraction of the failures. In other words, this model accounts for premature tensile failure in the regions close to the fiber ends. Detailed descriptions of the end-effect model and the nature of end-effects have been published previously by Stoner *et al.* [9]. Although all fibers are susceptible to end effects, fibers tested at longer gauge lengths are less likely to fail as a result of such effects.

Clearly, end effects do not constitute a specific flaw population, yet the flexible nature of the Weibull distribution enables it to be used to represent failures caused by end effects. However, the exact functional form of the distribution must be slightly different from those considered previously. Because only the region of the fiber near the glue spot is subject to end effects, there can be no direct gauge length dependence in the end effect survival function. If the total number of chain links subject to end effects is taken to be δ , then the probability of a fiber surviving end effects at a given stress level becomes

$$S_E = \exp\left(-\delta\left(\frac{\sigma}{\sigma_{0_E}}\right)^{m_E}\right) \quad (13)$$

The inclusion of the δ term would appear to increase the number of parameters to be fit from two to three. However, neither δ nor σ_{0_E} can have any gauge length dependence, provided that $L > \delta$. This implies that neither parameter can be determined independently of the other. Thus, they can be merged into a single empirical parameter, which will still be called σ_{0_E} for the sake of simplicity.

A fiber must survive both end effects and its flaw population or else it will fail, so the survival relation-

ship for the fiber becomes

$$S = S_F \cdot S_E \quad (14)$$

In this development, the subscripts F and E are used instead of the previously used 1 and 2 to distinguish between failures resulting from intrinsic flaws within the fiber (F) and those resulting from end effects (E). Survival of the inherent flaws within the fiber still assumes the form

$$S_F = \exp\left(-L\left(\frac{\sigma}{\sigma_{oF}}\right)^{m_F}\right) \quad (15)$$

It is important to realize that the length of fiber subject to end effects (δ) may also contain fiber flaws. Thus, the correct gauge length in eqn (15) remains L rather than $L - \delta$. The total survival relationship becomes

$$S = \exp\left(-L\left(\frac{\sigma}{\sigma_{oF}}\right)^{m_F} - \left(\frac{\sigma}{\sigma_{oE}}\right)^{m_E}\right) \quad (16)$$

while the probability of fiber failure becomes

$$F = 1 - \exp\left(-L\left(\frac{\sigma}{\sigma_{oF}}\right)^{m_F} - \left(\frac{\sigma}{\sigma_{oE}}\right)^{m_E}\right) \quad (17)$$

The shape and scale parameters can be determined by subjecting a given fiber sample to single-filament testing at multiple gauge lengths. However, the evaluation of shape and scale parameters is far more complex for the mixed-mode models than for the simple Weibull case, because the four parameters cannot be linearized. For non-linear equations, the approach commonly used to evaluate parameters is the method of maximum likelihood [9,11].

The application of maximum likelihood theory in fitting mixed-mode Weibull distributions was developed in detail by Stoner [9]. Modifications of programs developed by Stoner were used in this study to determine the four Weibull parameters (σ_{oF} , σ_{oE} , m_F and m_E).

Essentially, maximum likelihood theory evaluates the probability that a given set of tensile strengths would have resulted from a specific set of Weibull parameters. The strength distribution and form of the equations are provided, while the parameters are systematically varied to maximize the relative likelihood that the observed strength distribution resulted from the parameters. Derivations of the equations used in maximum likelihood theory can be found in the previously mentioned work by Stoner [9], or in the book by Everitt and Hand [12].

2. EXPERIMENTAL PROCEDURE

Both batches of PBO fibers used in this study were supplied by the Dow Chemical Company. The first batch of fibers (PBO-1) was produced during 1991, while the second batch (PBO-2) was produced during 1992. Table 2 details the properties of these fiber batches.

Table 2. Properties of as-received PBO fibers

Fiber Type	Year Produced	Average Diameter (μm)	Tensile Strength (GPa)	Tensile Modulus (GPa)
PBO-1	1990	16.0	3.38	151
PBO-2	1991	11.6	3.61	146

2.1 Evaluation of fibers

Tensile strengths and moduli of the carbonized and as-received fibers were determined by single-filament tensile testing, using an Instron model TM universal testing machine that had been modified and upgraded, by Measurement Technology, Inc. Unless otherwise specified, all single filament tensile tests employed 25 mm tabs and followed the procedure put lines in ASTM Standard D-3379-75 [13]. For the Weibull study, gauge lengths of 10, 25 and 40 mm were used. Fiber diameters were measured with a laser diffraction technique that is accurate to $\pm 0.1 \mu\text{m}$. Fifty single filaments were tested from each fiber set to determine average tensile values. In the Weibull study, a minimum of 71 single filaments were tested at each gauge length for each sample.

A four-point probe technique, similar to that described by Coleman [14], was used to determine the electrical resistivities of the carbonized PBO fibers. Fifteen single filaments were tested from each sample to determine its mean resistivity.

2.2 Batch carbonization

PBO fibers were cut with ceramic scissors into lengths of approximately 20 inches per sample. The samples were placed into the hearth of a graphite resistance furnace. The furnace temperature was measured with a Raytec pyrometer, which provided output to a Northrup Electromax programmable controller.

After placing the sample in the hearth, the furnace was sealed, and a series of evacuations were performed. First, a vacuum was drawn on the chamber. Then, the furnace was filled with a noble gas. This cycle was repeated several times to minimize the quantity of oxygen present in the furnace.

The fully evacuated furnace was filled with the noble gas to a positive pressure of approximately five psi. Next, the furnace was heated at this pressure to the desired temperature, held for the selected soak duration at the maximum temperature, then allowed to cool. For all batch trials in which soak duration was not the variable of interest, a 15 minute soak duration was employed.

2.3 Continuous carbonization

Continuous carbonization was performed in the same graphite resistance furnace as batch carbonization. In this mode, 18 inch long steel doors were connected to the end of the furnace. These doors were surrounded by cooling water coils. The fiber was fed from a winder, through the doors and body of the furnace, then connected to a bobbin on the

take-up winder. The ends of the doors were sealed by placing an end-cap across the opening and a vacuum was drawn on the entire system. The differential pressure created by the vacuum held the end-cap in place. After approximately 45 minutes, helium was passed through the system at a net positive pressure. The pressure forced the end-caps to fall off leaving the ends of the furnace open. The flowing helium prevented oxygen from seeping into the furnace and oxidizing the graphite.

The furnace was heated to the set-point temperature and the winders were activated. Tension was controlled by a take-up winder. Winding speed was determined from the revolution rate of the winder and the diameter of the bobbin. The length of fiber that was in the hot zone during the heating of the furnace was subjected to a significantly different thermal history from that of the rest of the fiber. Therefore, the first 12 inches of carbonized fiber were discarded.

3. RESULTS AND DISCUSSION

3.1 Nitrogen release

If nitrogen is primarily responsible for the decline in tensile strength observed when PBO fibers are heated in batch mode to temperatures greater than 1400°C, then any processing modifications that minimize the influence of this release should directly enhance the tensile strength of the carbonized fiber. The thermally induced release of nitrogen that disrupts the developing crystalline structure cannot be prevented. However, the relative crystallinity of the fiber at the time of release can be controlled.

If large graphite crystallites have formed prior to the release of nitrogen, the disruption of the structure will be substantial. However, if only small crystallites were present, the damage would be less severe, and the resultant fiber should maintain more of its inherent tensile strength. For a given maximum treatment temperature and soak duration, the heating rate is the primary factor controlling the development of crystallites. At lower heating rates, comparatively larger crystallites will form, while at high heating rates, the combination of enhanced nucleation and shorter growth times results in the formation of smaller crystallites [7].

The influence of heating rate was examined by carbonizing PBO-2 fibers in a batch mode at different heating rates. The rates varied from 1°C per minute to 60°C per minute, which was the maximum capacity of the furnace. Figure 2 shows that rapid heating rates led to substantially improved tensile strengths. Fibers heated at 60°C per minute developed more than three times the tensile strength of those heated at 1°C per minute. This supports the nitrogen release hypothesis.

The most rapid heating rates can be achieved by heat treating the fiber in a continuous fashion. In this mode of operation, the fiber is pulled at a constant rate through a heated furnace. The effective heating

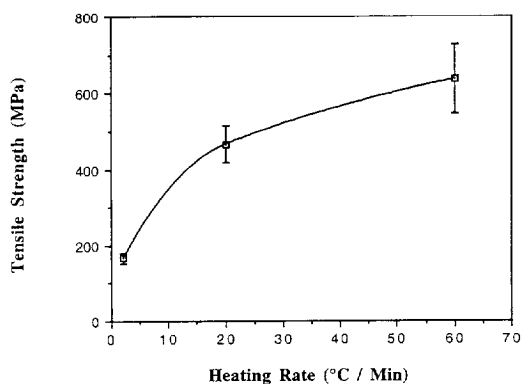


Fig. 2. Influence of heating rate on tensile strength of unstabilized PBO fibers heat-treated to 1800°C without tension.

rate in continuous operation is several orders of magnitude larger than the maximum 60°C per minute rate at which batch experiments could be performed. Therefore, fibers carbonized in a continuous fashion should be far less susceptible to nitrogen damage than those produced in a batch operation.

Figure 3 indicates the dramatic improvement in tensile strength resulting from continuous operation. A nearly two-fold increase in the tensile strength occurred, and the sharp drop in properties occurring above 1400°C was reduced considerably. More intriguingly, the development of electrical resistivity differed significantly for the fibers produced in continuous operation. Figure 4 shows that the electrical resistivity of fibers produced in a continuous fashion decreased monotonically with increasing treatment temperature and avoided the plateau observed in batch processing. This behavior indicates that the disruption of molecular order that affected the resistivities of fiber carbonized in a batch mode was eliminated when the fibers were heated in a continuous operation.

The electrical resistivity of PBO-based carbon fibers produced in a continuous operation at 2200°C was found to be approximately 9 $\mu\Omega$ m. This value is lower than that for most carbon fibers produced from polymeric precursors. Additionally, the resistivity

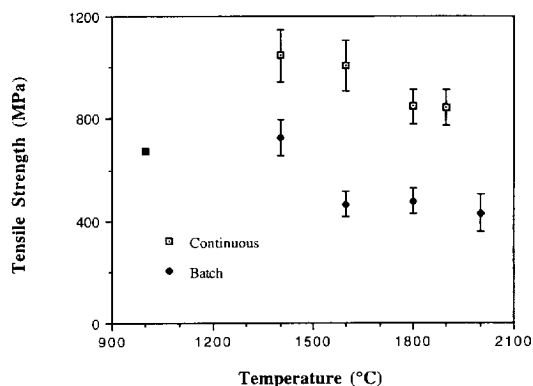


Fig. 3. Tensile strength of carbonized PBO fibers produced in batch and continuous operation.

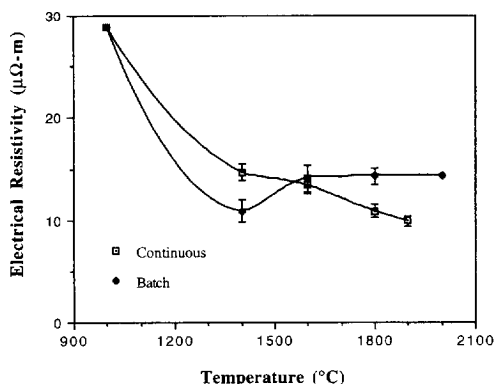


Fig. 4. Electrical resistivities of carbonized PBO fibers produced in batch and continuous operation.

places PBO in the conductivity range of some commercial mesophase pitch-based fibers. The low resistivities achieved by PBO-based fibers, coupled with their exceptional processibility, make PBO an attractive precursor possibility for the production of low-cost, high-thermal conductivity carbon fibers.

Although continuous operation provides substantially higher heating rates than batch operation, heating rate is not the only variable affected. Because the tow is pulled through the furnace in continuous operation, the fibers are always under tension. Therefore, the effects of tension must be examined to determine whether heating rate or tension was primarily responsible for the improved properties.

To isolate this effect, unstabilized PBO-2 fibers were heated to 1600°C at a rate of 20°C per minute under various levels of tension. Figure 5 indicates that tension provided only a minimal enhancement to the tensile properties of the carbonized fiber. Clearly, the results of these experiments indicate that heating rate is the primary cause of the enhanced tensile properties of continuously carbonized PBO fibers, and that the tension on the two provides only a minimal secondary enhancement of the tensile strength.

It is important to realize that not all of the damage occurs instantaneously or at a single temperature.

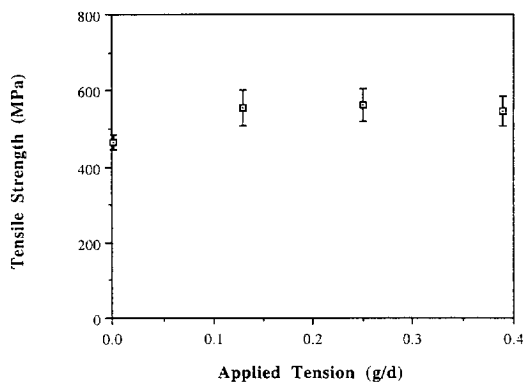


Fig. 5. Influence of applied tension on unstabilized PBO fiber heat-treated to 1800°C at a rate of 20°C min⁻¹.

Because of this, any nitrogen that remains in the fibers will further disrupt the structure if the fiber is exposed to the final heat treatment temperature for a longer time or if the fiber is exposed to a higher treatment temperature. Even fibers produced in a continuous operation may retain some of their nitrogen. Therefore, if continuously carbonized fibers were placed back in the furnace and heated in batch mode to the same temperature that they had experienced during continuous carbonization, some additional damage should result.

To test this hypothesis, four samples of PBO-2 fibers were continuously carbonized at different temperatures (1400, 1600, 1800 and 1900°C). Then, a portion of each sample was reheated in a batch operation to the same temperature to which it had been originally carbonized continuously. The fibers were heated at a rate of 20°C per minute to the temperature at which they had been continuously carbonized and allowed to remain at the maximum temperature for 10 minutes.

Table 3 shows that PBO-based fibers reheated in such a manner suffered a decrease in tensile strength until 1900°C. Fibers initially heated to temperatures above 1900°C did not experience this decline, possibly because their supply of bonded nitrogen had been exhausted during the initial continuous carbonization. This provides further indirect evidence that the decline in tensile strength is a result of the crystallite disruption caused by nitrogen release, rather than a simple function of the development of a graphitic structure. Collectively, these experiments provide evidence that nitrogen release is primarily responsible for the sharp decrease in tensile strength displayed by fibers carbonized in a batch mode.

3.2 Application of the Weibull distribution to PBO fibers

The strongest of the PBO-based carbon fiber samples was selected for further analysis. The Weibull models can be used to gain insight into the failure mechanisms of PBO-based carbon fibers. By applying the models to both the carbonized and as-received fiber, the changes in the flaw character of the fiber created by carbonization can be evaluated. These changes may provide insight into the carbonization process itself.

Fiber samples of both as-received and carbonized

Table 3. Tensile strength comparison for batch, continuous, and reheated fibers

Treatment Temperature (°C)	Tensile Strength (MPa)		
	Batch	Continuous	Reheated
1000	653	656	—
1400	725	1046	853
1600	465	1008	930
1800	515	846	801
1900	—	844	906
2000	432	—	—

PBO were tested at three different gauge lengths (10, 25 and 40 mm), using the standard single filament test techniques described in the experimental procedure section. The carbonized fiber used in this study had been heat treated without stabilization to 1400°C in a continuous process. Table 4 summarizes the properties of the fiber batches examined in this study.

Figure 6 shows the results of the linear regression of the Weibull function performed at each gauge length for the carbonized PBO fibers. In all three cases, the regressed line provided an excellent fit of the experimental data at individual gauge lengths. However, the slopes of these lines clearly differed. This implies that the simple Weibull distribution may not be sufficient to describe the observed tensile failure. Table 5 confirms that the shape and scale parameters varied significantly when the simple Weibull distribution was applied to data taken at each of the three gauge lengths.

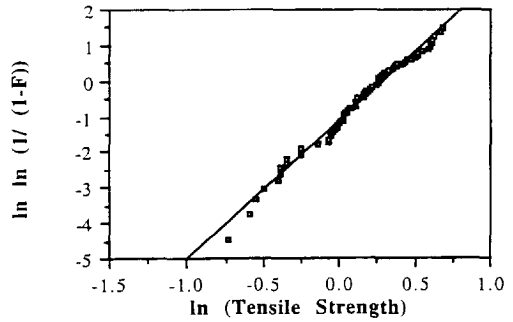
The concurrent and end-effect models were applied to both the carbonized and as-received fiber data. Table 6 summarizes the results of this analysis. Figure 7 shows a plot of the actual survival percentages versus those predicted by the concurrent model that provides evidence that the concurrent model is not appropriate for representing the tensile failure data. The figure shows that while the concurrent model provides an excellent representation of the 40 mm carbonized fiber data, the model deviates somewhat from the 25 mm gauge length data, and the model provides a poor representation of the 10 mm gauge length data. Thus, the concurrent model does not accurately represent the physical situation, and a model in which one failure mechanism does not depend on gauge length, such as the end-effect model, must be considered.

Figure 8 compares the survival fractions predicted by the end-effect model to both those predicted by the simple Weibull model and those determined experimentally. Analysis of variance shows that, when applied across all three gauge lengths, the end-effect model provides a more accurate representation of the observed tensile data than either the concurrent or simple Weibull models. This is primarily a result of the improved predictions of failure at 10 mm gauge lengths.

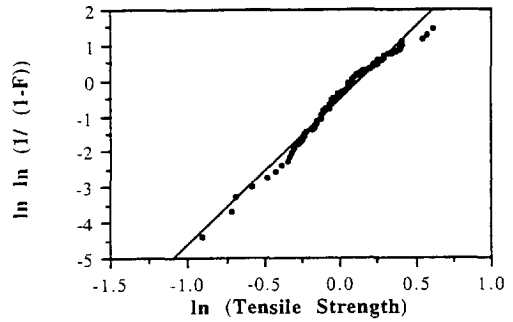
The influence of true flaws and end effects can be

Table 4. Properties of tested fibers

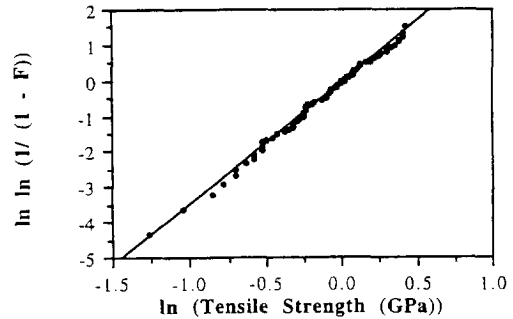
Gauge Length (mm)	Number of Fibers	Average Diameter (μm)	Tensile Strength (MPa)
Carbonized			
10	82	9.5 ± 0.2	1225 ± 84
25	80	9.5 ± 0.1	1051 ± 69
40	76	9.7 ± 0.2	933 ± 74
As-Received			
10	74	11.7 ± 0.2	3768 ± 161
25	71	11.6 ± 0.2	3625 ± 178
40	75	11.4 ± 0.2	3035 ± 165



(a)



(b)



(c)

Fig. 6. Simple Weibull distribution applied to carbonized fibers of different gauge lengths.

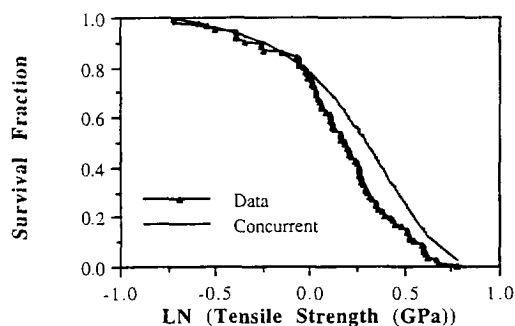
Table 5. Shape and scale parameters for carbonized PBO fibers

Gauge Length (mm)	Shape Parameter (m)	Scale Parameter (σ ₀)
10	3.87	1.74
25	4.09	2.49
40	3.44	3.00

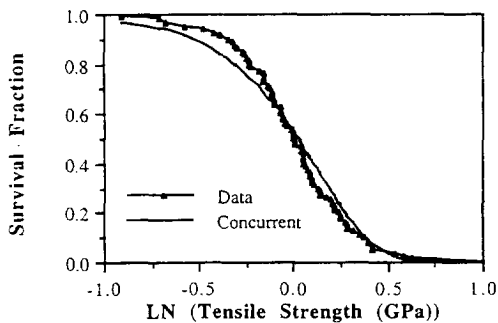
separated with this model. Because separate shape and scale parameters are calculated for flaws and end effects, the probability of failure resulting from either failure mode can be predicted. Figure 9 shows that true flaws dominate the failure at 40 mm gauge lengths, while end effects exert more influence at smaller gauge lengths. This is consistent with the basic assumptions of the end-effect model. Because

Table 6. Summary of Weibull parameters

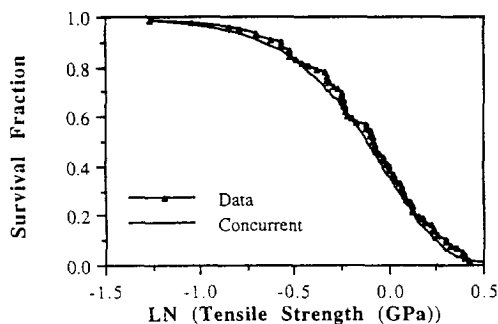
	σ_{o1}	$m_1(m_F)$	σ_{o2}	$m_2(m_E)$
Carbonized				
Concurrent	3.815	3.351	3.544	3.750
End-Effect	3.670	3.168	1.580	3.374
Simple	2.986	3.340	—	—
As-Received				
Concurrent	18.573	3.188	10.968	3.820
End-Effect	13.159	3.129	4.971	2.998
Simple	10.395	3.188	—	—



(a)



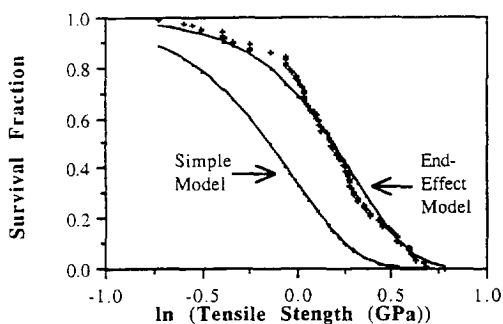
(b)



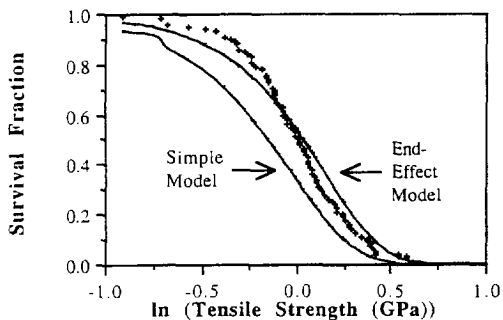
(c)

Fig. 7. Concurrent model applied to carbonized fibers of different gauge lengths.

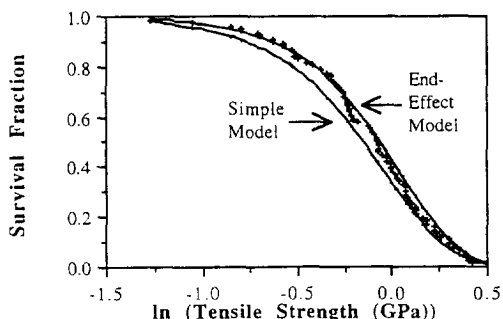
the end effects are independent of gauge length, they should result in the same failure probability at different gauge lengths. At small gauge lengths, the probability of a fatal flaw existing in the fiber itself is less than at large gauge lengths. Thus, end effects



(a)



(b)



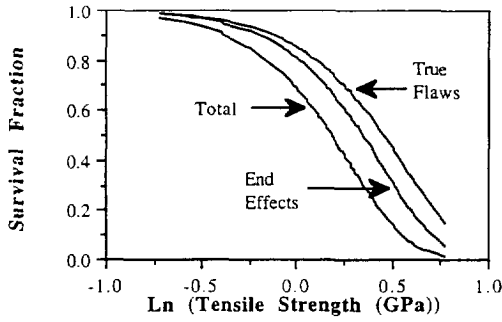
(c)

Fig. 8. Comparison of end-effect and simple models for carbonized PBO fiber at various gauge lengths.

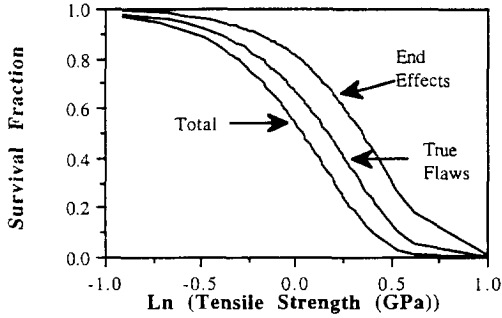
should result in more failures at small gauge lengths than at large ones, simply because there is a higher probability of the fiber surviving its flaws at a high enough stress to fail as a result of end effects.

Surprisingly, similar trends were observed when the as-received PBO fibers were subjected to single-filament testing. The concurrent distribution misrepresented the survival fraction at low gauge lengths, again implying that both a gauge-length-dependent and a non-gauge-length-dependent failure mechanism were involved. Also, the end-effect model again provided a superior fit across all gauge lengths, when compared to either the simple Weibull or concurrent models. Finally, as before, the importance of end effects decreases as gauge length increases. These results are summarized in Figs 10–12.

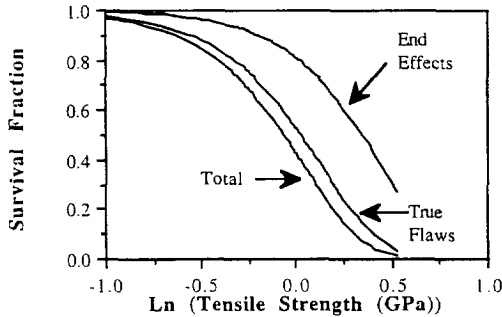
Earlier in this paper, carbonization and the struc-



(a)



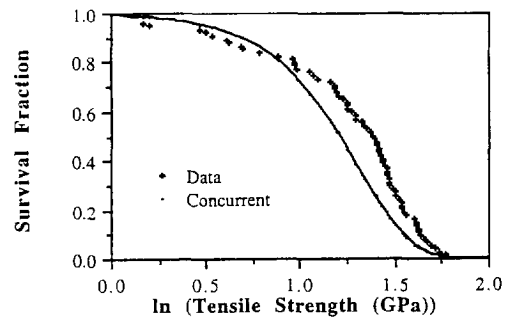
(b)



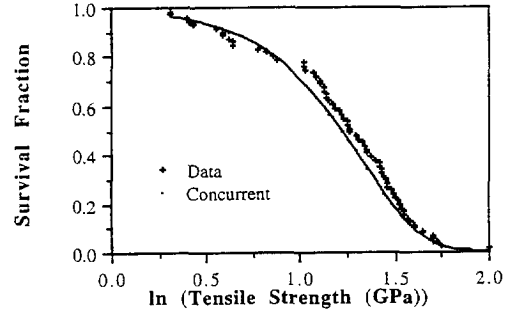
(c)

Fig. 9. Contribution of end effects and true flaws on carbonized PBO fibers of different gauge lengths.

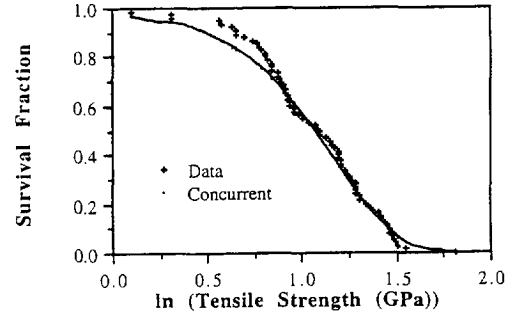
tural damage that this process generated within the fiber were discussed in detail. Based on this discussion, one might expect that this structural damage would create a new flaw population in the fiber. Failure in the carbonized fiber then would occur as a result of a combination of flaws present in the precursor and flaws created during carbonization. However, this was not observed for carbonized PBO fiber. Instead, both the carbonized and as-received fibers appear to fail by the same combination of end effects and true flaws. Two possible explanations exist for this surprising result. Either the effects of the original flaw distribution in the as-received fiber are dwarfed by both end effects and carbonization flaws, and thus they can be essentially ignored, or the flaws induced during carbonization are a reflection of flaws in the precursor material.



(a)



(b)

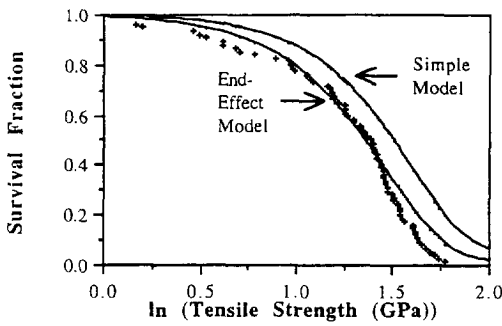


(c)

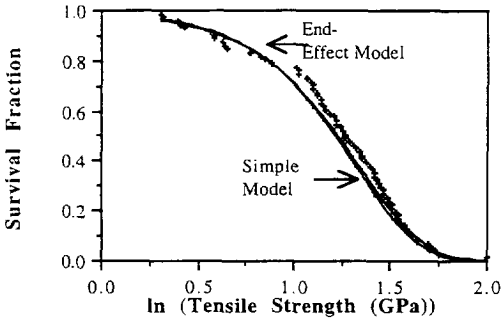
Fig. 10. Concurrent model applied to as-received fibers of different gauge lengths.

If the flaws in the carbonized fiber are controlled by the flaws in the as-received fiber, then the shape factor for the two distributions should be the same. In this case, the gauge length dependent term (m_F) of the end-effect model should be the same for the carbonized and the as-received fiber. However, the scale factor (σ_{oF}) could vary. This parameter is a function of the severity of the flaws, and carbonization might be expected to increase flaw size.

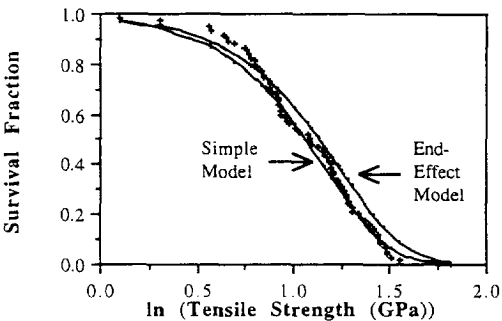
Table 6 shows that, when the end-effect model was applied, the shape factor was found to be 3.168 for the carbonized fiber and 3.129 for the as-received fiber. Clearly these values are similar, which alone would imply a relation between the distributions. However, one cannot conclude that the same flaw distribution is regulating both fiber types unless the values do not differ statistically. This requires the



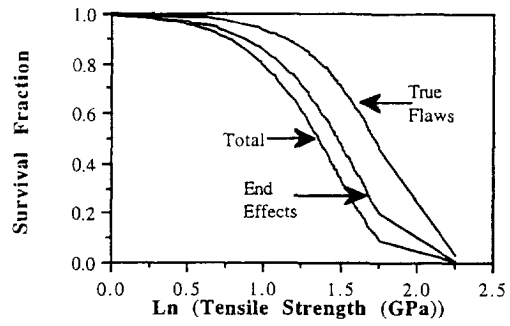
(a)



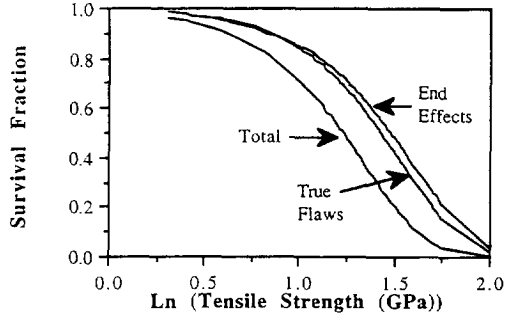
(b)



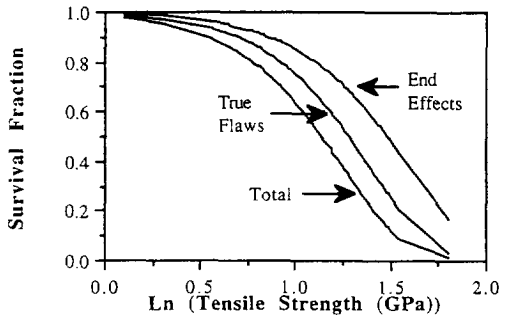
(c)



(a)



(b)



(c)

Fig. 11. Comparison of end-effect and simple models for as-received PBO fiber at various gauge lengths.

Fig. 12. Contribution of end effects and true flaws on as-received PBO fibers of different gauge lengths.

calculation of confidence intervals. The method for determining confidence intervals for multiple term regressions through point variances is discussed by Pfaffenberger and Patterson [15]. Using this approach, 95% confidence intervals were determined for the regression parameters.

As Fig. 13 shows, the 95% confidence intervals for the as-received and carbonized fibers overlap. Therefore, the regressed values for m_1 for the as-received and m_F for the carbonized fibers are statistically indistinguishable. This implies that the same flaw distribution is controlling the failure in both fiber types. Thus, the flaws induced during spinning appear to be directly related to the flaw population in the carbonized fiber. In fact, it would appear that carbonization merely increases the sever-

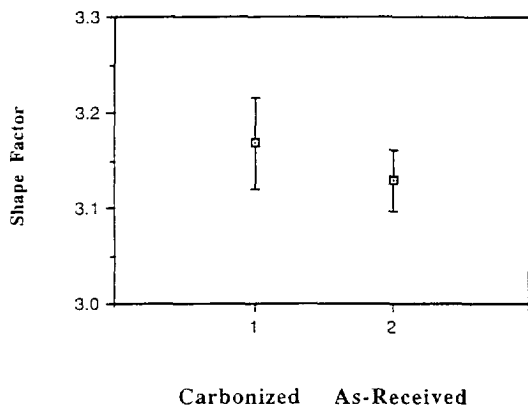


Fig. 13. Confidence intervals for regressed shape factor values for carbonized and as-received PBO fibers.

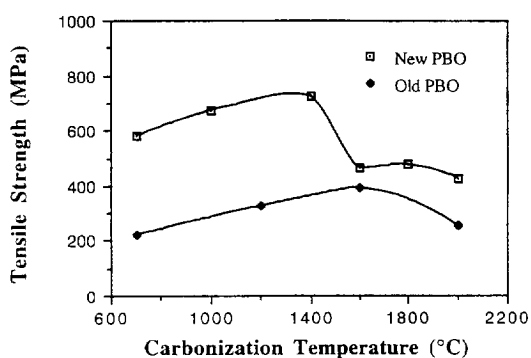


Fig. 14. Tensile strength comparison for carbon fiber made from unstabilized old (PBO-1) and new (PBO-2) fiber in batch operation.

ity of existing flaws found in the as-received PBO fibers.

To further support this assertion, an older batch of PBO fibers was obtained and tested. The properties of this older batch of PBO (denoted as PBO-1) are compared to those of the PBO fiber used in the other portion of this study this study (PBO-2) in Table 2. Figure 14 shows the tensile strengths of carbon fibers made from these two PBO batches. The carbon fibers produced from the newer PBO-2 possessed dramatically superior tensile strengths to those produced from the older PBO-1. This implies that further improvements in the quality of the precursor fibers may lead to higher tensile strengths in the carbonized fibers.

4. CONCLUSIONS

This work has shown that the tensile strength of PBO-based carbon fibers is limited by flaws present in the precursor fiber. A point variance analysis of the end-effect Weibull model shape parameters indicates that the flaw distribution present in the polymeric fiber is statistically indistinguishable from the flaw distribution which results in tensile failure in the carbonized fiber. Thus, enhancements in the polymer spinning process led to improved tensile strength in the carbonized fiber. Also, the release of nitrogen

during crystallite growth led to a reduction in the tensile strength of the carbon fibers. However, the damage caused by this nitrogen release can be minimized by heating rapidly through the region of nitrogen release. Therefore, the rapid heating rates associated with the continuous carbonization of PBO fibers provides the most economical means of conversion and the best balance of properties.

Acknowledgements—The authors would like to thank the Dow Chemical Company, Midland, Michigan for supporting this work. The authors would also like to thank David Johnson of the University of Leeds for his critical discussions of the flaw and failure aspects of this paper.

REFERENCES

1. J. R. Glatz, M. A. Kinna and W. C. Riley, *DOD Metal Matrix Composites Information Analysis Center Current Highlights*, **8**, 1 (1988).
2. J. A. Newell, D. K. Rogers, D. D. Edie and C. C. Fain, *Carbon* **32**, 651 (1994).
3. E. Fitzer, *Carbon* **27**, 621 (1989).
4. E. Fitzer and W. Frohs, *Carbon* **88**, p. 298. Newcastle upon Tyne, UK (1988).
5. E. Fitzer, W. Frohs, and G. Liu, *Supplement to the Proceedings, Carbon 86*, p. 873. Baden-Baden, Germany (1986).
6. D. K. Rogers, S. P. Jones, C. C. Fain and D. D. Edie, *Carbon* **31**, 303 (1993).
7. D. J. Johnson, In *Chemistry and Physics of Carbon* (Edited by P. L. Walker, Jr), Vol. 20, pp. 1–58. Marcel-Dekker, New York (1987).
8. C. P. Beetz, *Fibre Sci. Technol.* **16**, 45 (1982).
9. E. G. Stoner, The Effect of Shape on the Tensile Strength of Pitch-Based Carbon Fibers, Ph.D. Dissertation, Clemson University, Clemson, SC (1991).
10. E. G. Stoner, D. D. Edie and S. D. Durham, *J. Mat. Sci.* **29**, 6561 (1994).
11. G. J. Hayes, Analysis of the Single Filament Recoil Test, Ph.D. Dissertation, Clemson University, Clemson, SC (1993).
12. B. S. Everitt and D. J. Hand, *Finite Mixture Distributions*. Chapman and Hall, Ltd, London (1981).
13. ASTM Standard D3379-75, (reapproved 1989).
14. L. B. Coleman, *Rev. Sci. Inst.* **46**, 1125 (1975).
15. R. C. Pfaffenberger and J. H. Patterson, *Statistical Methods*, Third Edition, Richard D. Irwin, Inc., Homewood, IL (1987).
16. *Amoco Performance Products*, Thornel Product Information Sheet, (1992).